Science Advances
AAAS

advances.sciencemag.org/cgi/content/full/7/3/eabd4235/DC1

Supplementary Materials for

TRAF6-IRF5 kinetics, TRIF, and biophysical factors drive synergistic innate responses to particle-mediated MPLA-CpG co-presentation

P. Pradhan, R. Toy, N. Jhita, A. Atalis, B. Pandey, A. Beach, E. L. Blanchard, S. G. Moore, D. A. Gaul, P. J. Santangelo, D. M. Shayakhmetov, K. Roy*

*Corresponding author. Email: krish.roy@gatech.edu

Published 13 January 2021, *Sci. Adv.* **7**, eabd4235 (2021)
DOI: 10.1126/sciadv.abd4235

This PDF file includes:

SUPPLEMENTAL INFORMATION

Supplemental Method

***Tlr4*$^{lps\text{-}del}$*/JthJ* mouse from Jackson Laboratory (**https://www.jax.org/strain/007227**)**: The stimulation of Toll-like receptor 4 (TLR4) by lipopolysaccharide (LPS) induces the release of proinflammatory cytokines that activate immune responses. The *Tlr4*$^{Lps\text{-}del}$ spontaneous mutation corresponds to a 74723 bp deletion that completely removes the *Tlr4* coding sequence. No mRNA or protein is expressed. Homozygous mutants exhibit a defective response to LPS stimulation. The functionally similar *Tlr4*$^{Lps\text{-}d}$ mutation found in C3H/HeJ mice (#000659) is a point mutation that causes an amino acid substitution.

TLR9$^{M7Btlr/MmJax}$ mouse from Jackson Laboratory (https://www.jax.org/strain/014534): Mice that are homozygous for this mutation are viable, fertile, normal in size and do not display any gross physical or behavioral abnormalities. In response to stimulation with oligodeoxynucleotides containing CpG motifs, macrophages do not produce tumor necrosis factor (TNF) alpha. This mutant mouse strain may be useful in studies of the role of toll like receptor 9 (TLR9) in the immune system.

Supplemental Table

Table S1. PLP formulations for MPLA and CpG

TLR adjuvants and Loading methods	**MP** formulations	**NP** formulations (Low density)	**NP** formulations (High density)
MPLA (M) *Encapsulation*	MLo MP *Density: 1.34E-06 mg/m3* *Loading: 1 ug MPLA /mg MP*	MLo NP *Density: 1.34E-06 mg/m3* *Loading: 1 ug MPLA /mg NP*	MHi NP *Density: 8.04E-06 mg/m3* *Loading: 6 ug MPLA /mg NP*
CpG (C) *Surface loading*	CHi MP *Density: 3.35 mg/m2* *Loading: 10 ug CpG /mg MP*	CLo NP *Density: 0.056 mg/m2* *Loading: 10 ug CpG /mg NP*	CHi NP *Density: 3.35 mg/m2* *Loading: 60 ug CpG /mg NP*
MPLA (M) + **CpG** (C) *Encapsulation - MPLA* *Surface loading - CpG*	MLo-CHi-Dual MP *Density and loading - same as MLo-MP and CHi-MP*	MLo-CLo-Dual NP *Density and loading - same as MLo-NP and CLo-NP*	MHi-CHi-Dual NP *Density and loading - same as MHi-NP and CHi-NP*
Dose of adjuvants- MPLA at 50 ng/ml and CpG at 500 ng/ml concentration *Dose ratio - MPLA:CpG is 1:10*			
Note, it was not possible to prepare MHi-CHi-Dual MP or MLo-CLo-Dual MP formulations that require co-loading of MPLA (by encapsulation) and CpG (by surface loading) on MPs at 1:10 weight ratio between MPLA and CpG (to maintain same adjuvant doses across MP and NP formulations) with 100% loading efficiency for both adjuvants to match adjuvant densities on the corresponding NP formulations. For our formulations, approximately 6-fold higher surface area for NPs (avg size – 250 nm) compared with MPs (avg size - 1.5 um) enables 6-fold higher surface loading of CpG on NPs with 100% efficiency. Typically, our MPs can surface load up to a maximum of 10 ug CpG/mg particle with 100% efficiency whereas NPs can load up to 60 ug CpG/mg particle with 100% efficiency due to 6X higher surface area. 100% loading efficiency of adjuvants is important to maintain the dose ratio between MPLA and CpG across experiments.			

Table S2. Size, polydispersity index, zeta potential and loading levels for PLP formulations

PLP formulations	**Size (nm)** (before PEI modification)	**Polydispersity index** (before PEI modification)	**Zeta (mV)** (after PEI modification)	**MPLA and/or CpG loading levels**
MLo MP	*1353.3 ± 154.5 (n=3)*	*0.407 ± 0.514 (n=3)*	*+28.9 ± 1.6 (n=3)*	*1 ug MPLA /mg MP*
CHi MP	*1114.6 ± 336.2 (n=3)*	*0.650 ± 0.330 (n=3)*	*+29.4 ± 3.2 (n=3)*	*10 ug CpG/mg MP*
MLo-Chi-Dual MP	*1353.3 ± 154.5 (n=3)*	*0.406 ± 0.514 (n=3)*	*+28.9 ± 1.6 (n=3)*	*1 ug MPLA and 10 ug CpG /mg MP*
MLo NP	*240.3 ± 4.8 (n=4)*	*0.125 ± 0.069 (n=4)*	*+28.5 ± 2.1 (n=4)*	*1 ug MPLA /mg NP*
CLo NP	*248.2 ± 31.2 (n=4)*	*0.113 ± 0.036 (n=4)*	*+29.1 ± 0.8 (n=4)*	*10 ug CpG/mg NP*
MLo-CLo-Dual NP	*240.3 ± 4.8 (n=4)*	*0.125 ± 0.069 (n=4)*	*+28.5 ± 2.1 (n=4)*	*1 ug MPLA and 10 ug CpG /mg NP*
MHi NP	*238.8 ± 35.3 (n=2)*	*0.082 ± 0.069 (n=2)*	*+26.3 ± 0.4 (n=2)*	*6 ug MPLA /mg NP*
CHi NP	*248.2 ± 31.2 (n=4)*	*0.113 ± 0.036 (n=4)*	*+29.1 ± 0.8 (n=4)*	*60 ug CpG/mg NP*
MHi-CHi-Dual NP	*238.8 ± 35.3 (n=2)*	*0.082 ± 0.069 (n=2)*	*+26.3 ± 0.4 (n=2)*	*6 ug MPLA and 60 ug CpG /mg NP*

Table S3. Encapsulation efficiencies for MPLA (synthetic MPLA-PHAD) or LPS in PLPs as measured by various analytical methods

Analytical methods	**MPLA/LPS formulations**	**Encapsulation efficiency percentage for MPLA or LPS (mean ± SD)**
LC-MS for MPLA	MLo MP	69.4 ± 28.3 (n=3)
	MLo NP	84.8 ± 4.6 (n=3)
	MHi NP	45.6 ± 10.5 (n=3)
GC-MS for MPLA	MLo MP	76 (n=1)
	MLo NP	76 (n=1)
	MHi NP	61.9 (n=1)
Fluorometry for LPS-FITC	LPSLo MP	39.7 ± 1.3 (n=3)
	LPSLo NP	66 ± 0.4 (n=3)
	LPSHi NP	47 ± 5.2 (n=3)

Table S4. Effect of particle size and density on cytokine responses of PLPs in BM-APCs

Biophysical parameters	IFN beta	IL-12p70	IL27	IL10	TNF alpha	IL6
Synergy for MPLA+CpG	*Yes*	*Yes*	*Yes*	*Yes*	*No*	*No*
Particle size	*No*	*No*	*No*	*No*	*Yes*	*Yes*
CpG density	*Yes*	*Yes*	*Yes*	*Yes*	*No*	*No*
MPLA density	*No*	*No*	*No*	*No*	*No*	*No*

Supplemental Figures

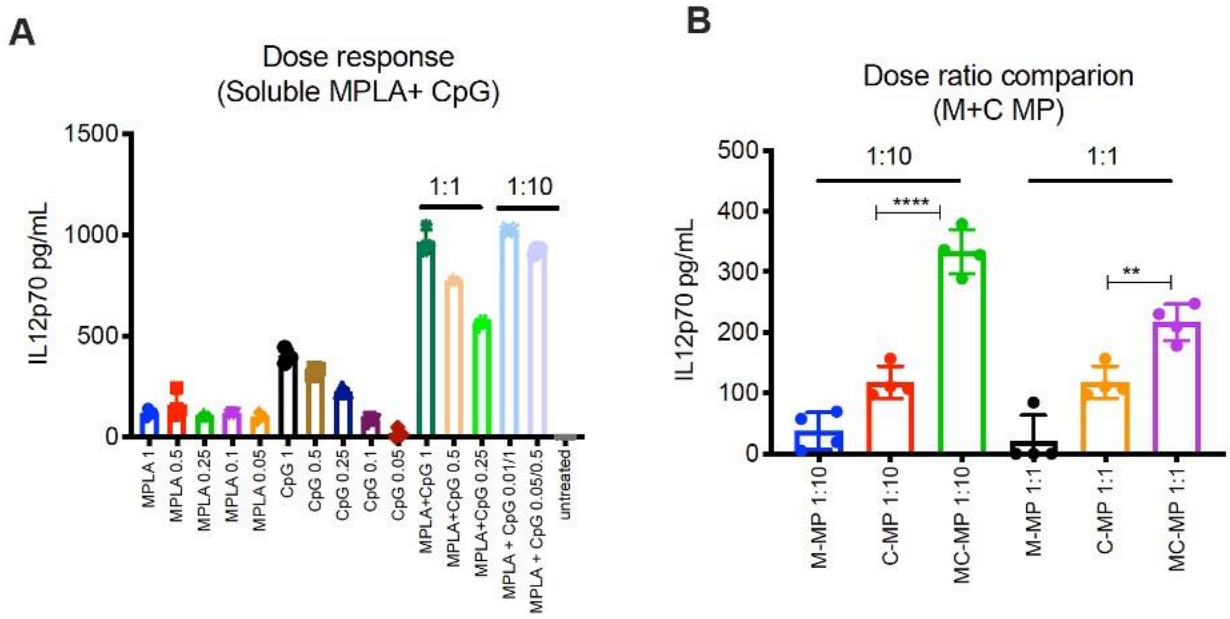

Figure S1. Effect of various doses and ratios of soluble and MP formulations of MPLA and CpG on IL-12p70 secretion by BM-APC's. Data represent Mean ± SD. **P < 0.01, ****P<0.0001, one-way ANOVA with Tukey's multiple comparison test.

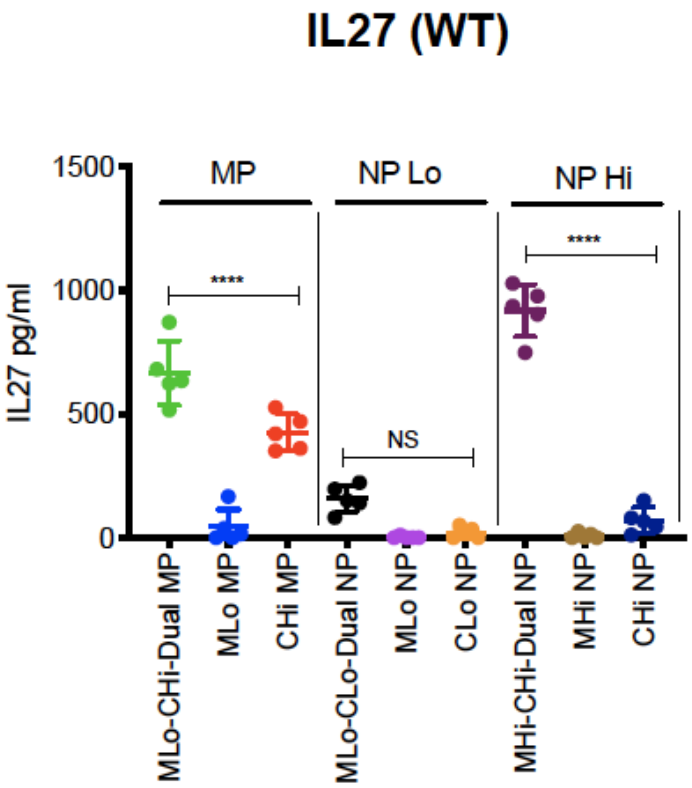

Figure S2. Synergistic IL27 response from BM-APCs induced by pathogen-like particles (PLPs) with MPLA and CpG depends on CpG adjuvant density. Center lines designate the mean value and error bars represent SD. ****P<0.0001, NS- not significant; one-way ANOVA with Tukey's multiple comparison test.

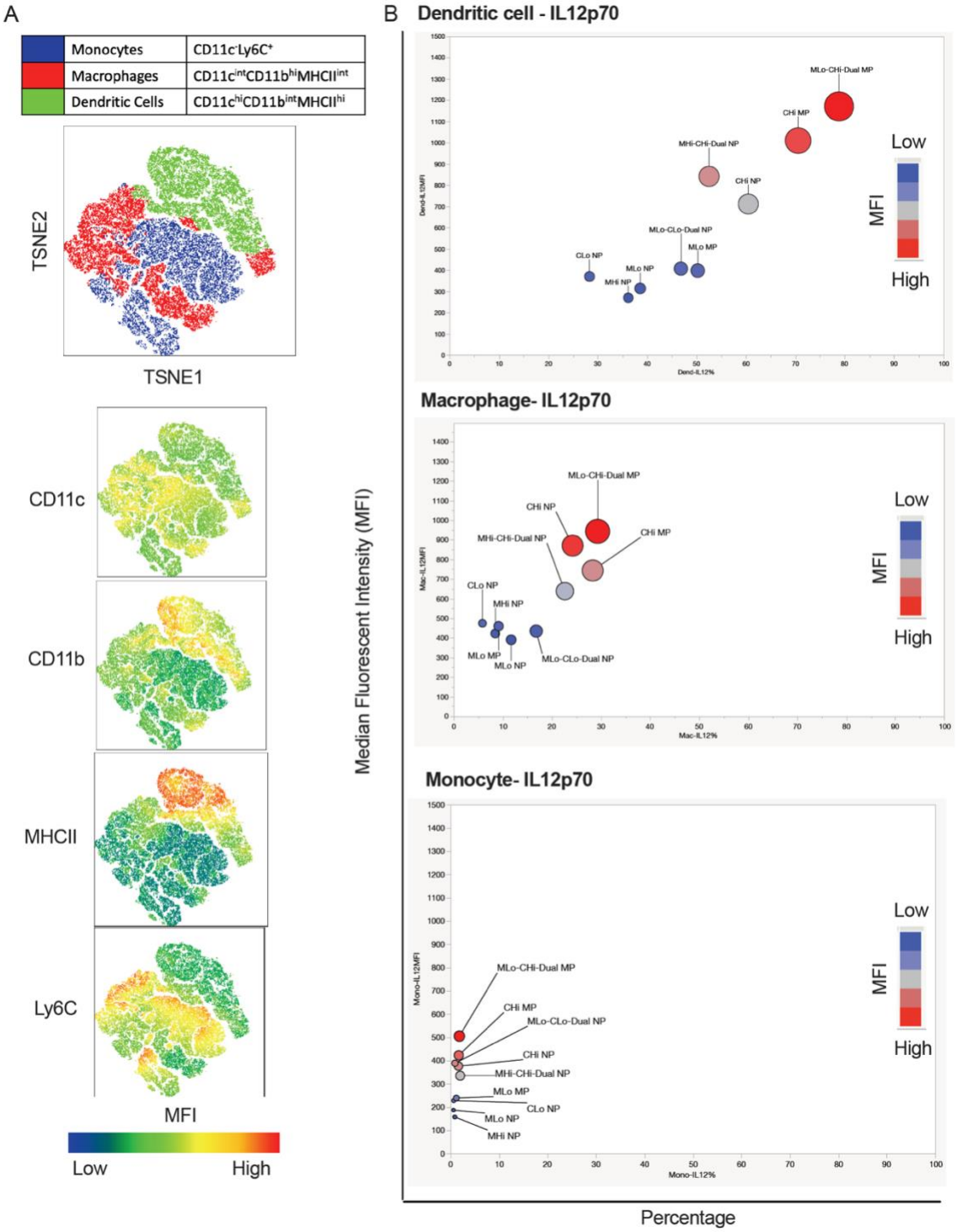

Figure S3. **Immune cell subsets in GMCSF-derived BM-APCs and their IL12p70 responses to PLPs**. Flow cytometry analysis of GMCSF-derived BM-APCs for A) cellular subsets and their b) IL12p70 response following 6-hr activation with various PLPs.

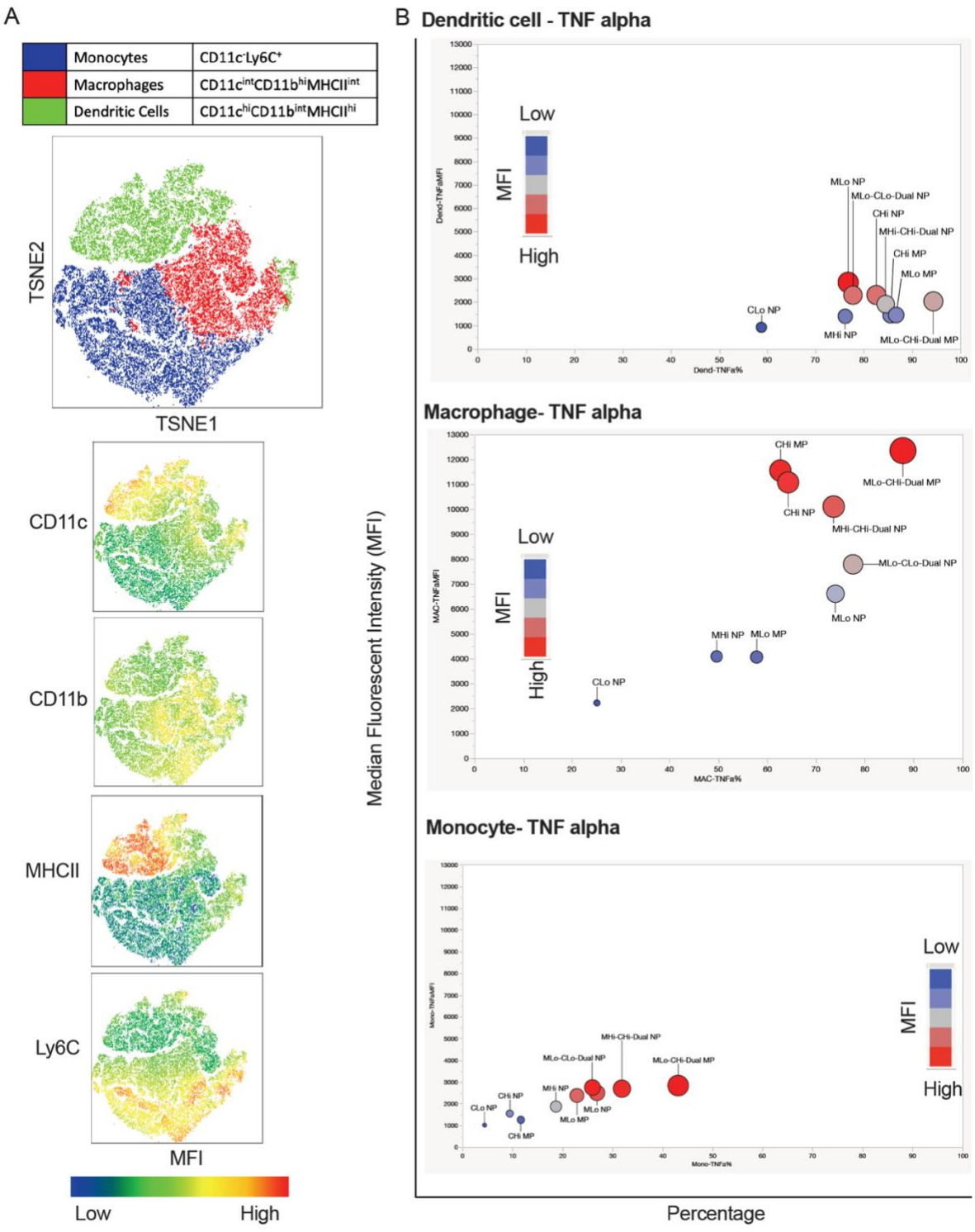

Figure S4. Immune cell subsets in GMCSF-derived BM-APCs and their TNF alpha responses to PLPs. Flow cytometry analysis of GMCSF-derived BM-APCs for A) cellular subsets and their b) TNF alpha response following 6-hr activation with various PLPs.

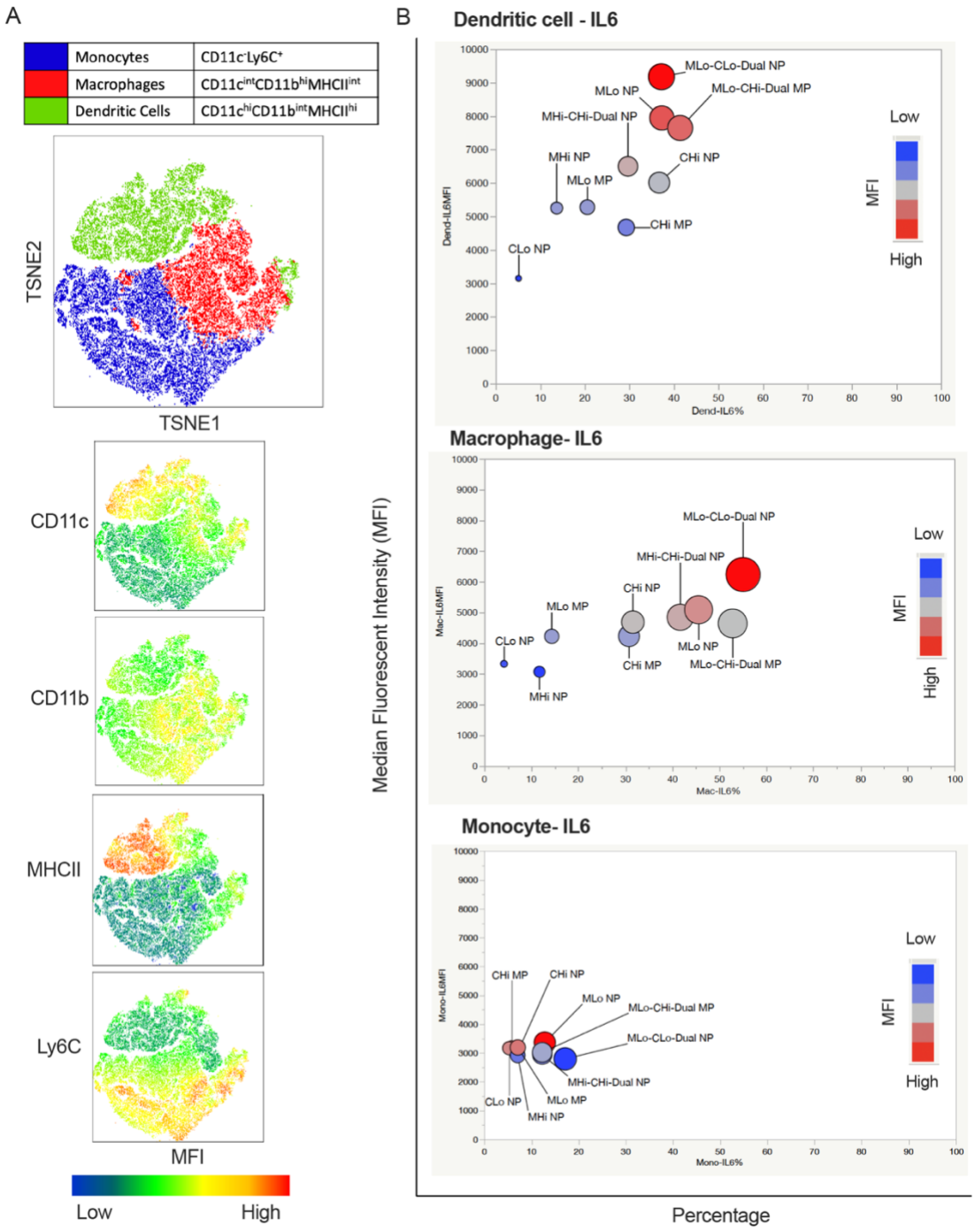

Figure S5. Immune cell subsets in GMCSF-derived BM-APCs and their IL6 responses to PLPs. Flow cytometry analysis of GMCSF-derived BM-APCs for A) cellular subsets and their b) IL6 response following 6-hr activation with various PLPs.

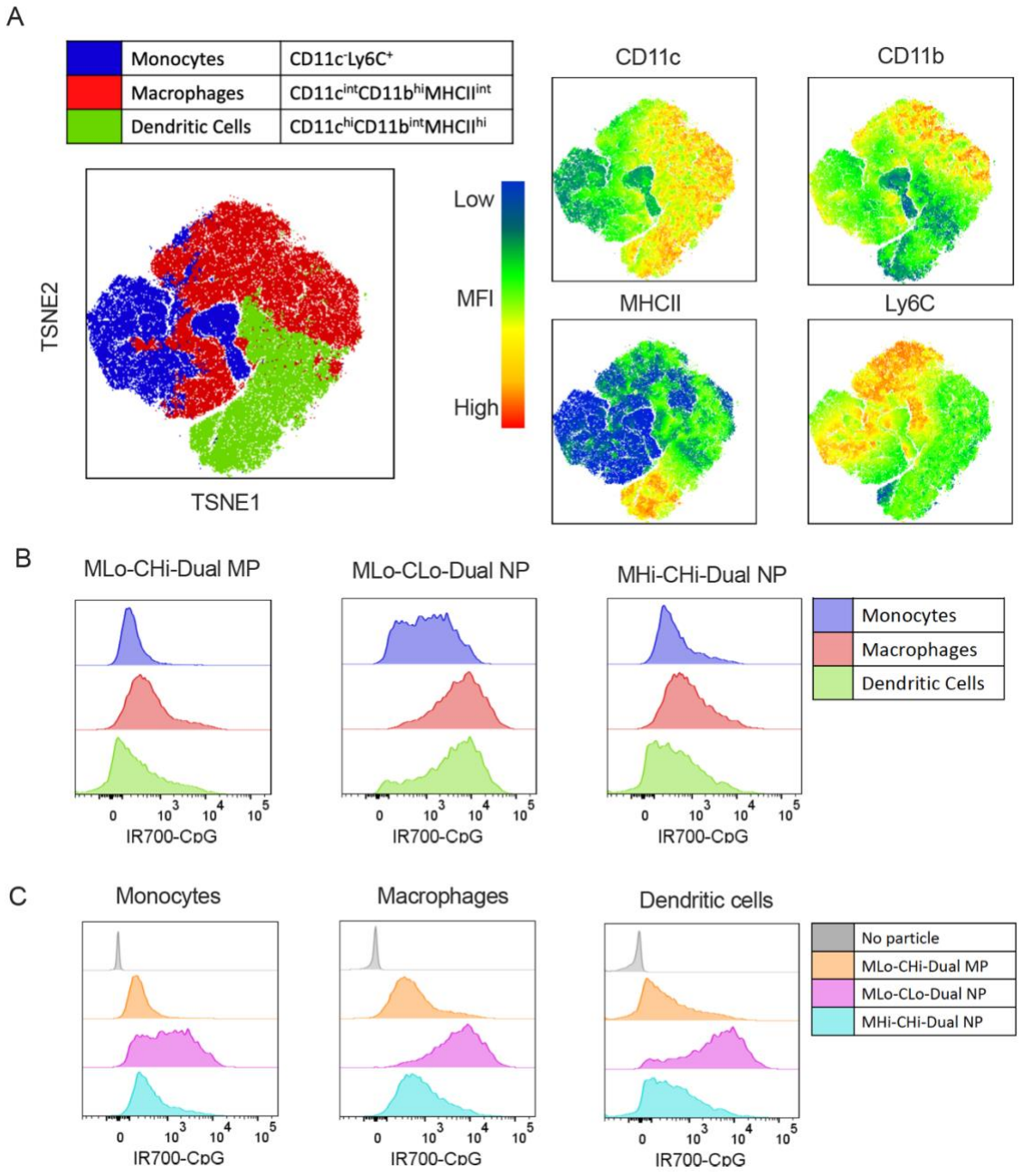

Figure S6. Differential uptake of PLPs by various immune cell subsets in GMCSF-derived BM-APCs. A) TSNE plots showing immune cell subsets and their surface marker expression; B-C) Flow histograms showing uptake of fluorescent CpG (IR700-CpG) surface loaded PLPs by monocytes, macrophages and dendritic cells following 24-hr incubation of PLPs with GMCSF-derived BM-APCs.

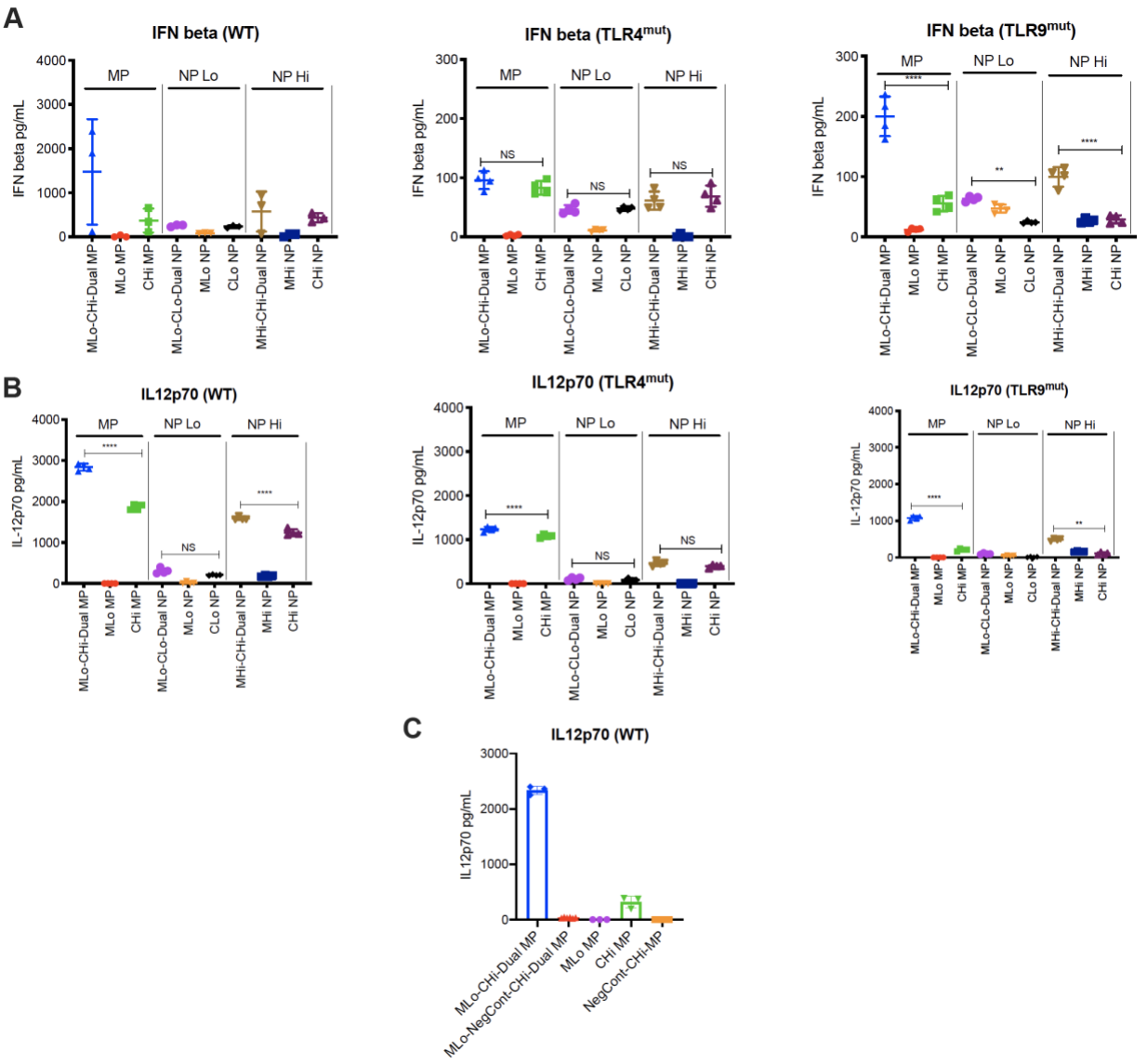

Figure S7. Effects of TLR4 and TLR9 signalings on the synergistic IFN-β and IL-12p70 responses of PLPs in BM-APCs. A) IFN-β and B) IL-12p70 secretion from BM-APC's after PLP treatment in wild-type, TLR4^{mut}, and TLR9^{mut} BM-APC's; C) IL12p70 levels in wild type BM-APCs following treatment with regular CpG (ODN 1826) or negative control CpG (ODN 2138) loaded PLPs. Center lines designate the mean value and error bars represent SD. **P < 0.01, ****P<0.0001, NS- not significant; one-way ANOVA with Tukey's multiple comparison test.

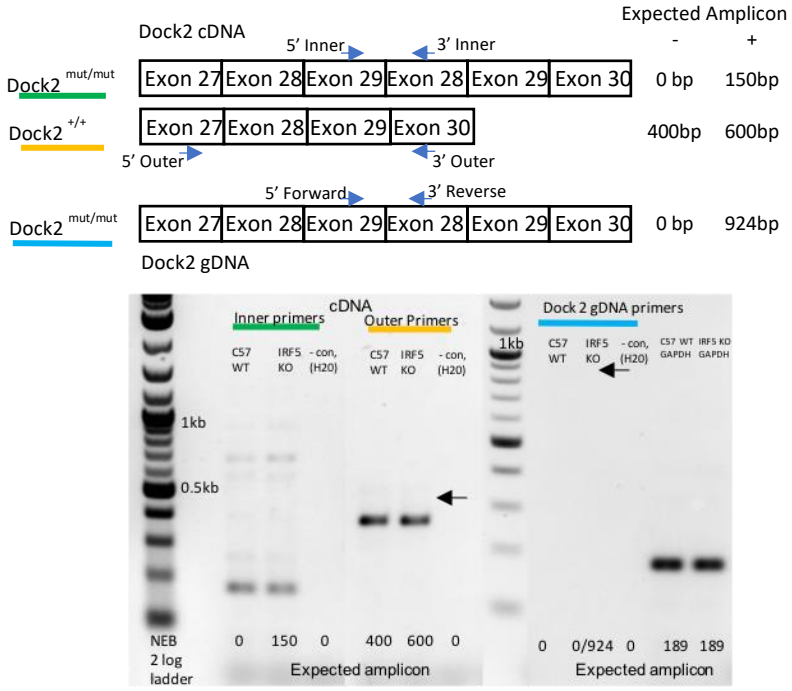

Figure S8. Possibility of DOCK2 mutation in our IRF5$^{-/-}$ mice colony. Amplicon was visualized via 1.5% agarose gel. **Lane 1**: NEB 2 Log ladder. **Lane 3 and 4**: Inner primers (spanning Exon 29 and 28) on cDNA flanking the DOCK2 mutation. An amplicon is visualized at 150bp in both wild type C57 and IRF5$^{-/-}$ samples. If there was DOCK2 mutation, then amplicon would only be seen in the IRF5$^{-/-}$. To reassess this amplicon, new gDNA primers were used to reassess this mutation (Lane 10 and 11). **Lane 6 and 7:** Outer primers (spanning Exon 27 and 30) on cDNA. Amplicon at 400 bp in conjunction with no amplicon at 600bp indicates no DOCK2 mutation in our IRF5$^{-/-}$ colony. **Lane 9:** NEB 2 Log ladder. **Lane 10 and 11:** new genotyping primers with gDNA for DOCK2 mutation in wild type and IRF5$^{-/-}$ mice. Lack of 924bp amplicon indicates no DOCK2 mutation in our IRF5$^{-/-}$ colony. This was reconfirmed with Purtha et al. *(38)*. All primers and schematic are adapted from Purtha et al. (*38*).

cDNA Primers:

Outer forward 27–30, 5′- GGATGCGGCCTTCACTTA-3′; and Outer reverse 27–30, 5′-TCCACAGCTGGAACTC- AAAG-3′.

Dock2 Mutation forward 29–28, 5′-CAAGGACCTCATTGGGAAGAA-3′; and Dock2 mutation reverse 29–28, 5′-CTGAGCTGGTCTGGAAGGTCT-3′

gDNA Primers- Dock 2 mutation forward: TCACTGCCCCTTAATGATGTC, Dock2 mutation reverse: TTGCCTTTGACACACCGTAG

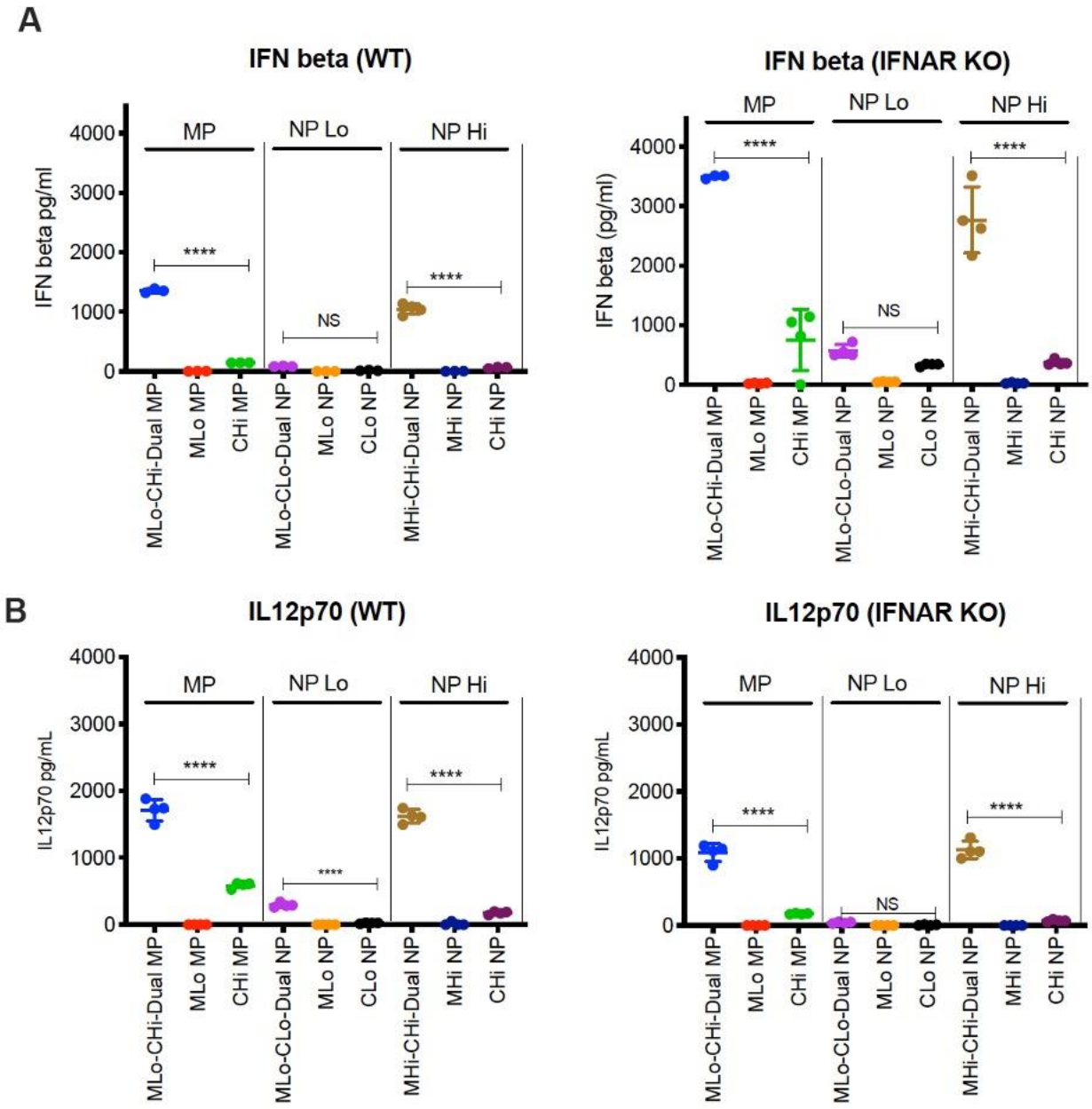

Figure S9. IFN-β and IL-12p70 secretion from BM-APCs after PLP treatment in wild-type and IFNAR knockout BM-APCs. Center lines designate the mean value and error bars represent SD. ****P<0.0001, NS- not significant; one-way ANOVA with Tukey's multiple comparison test.

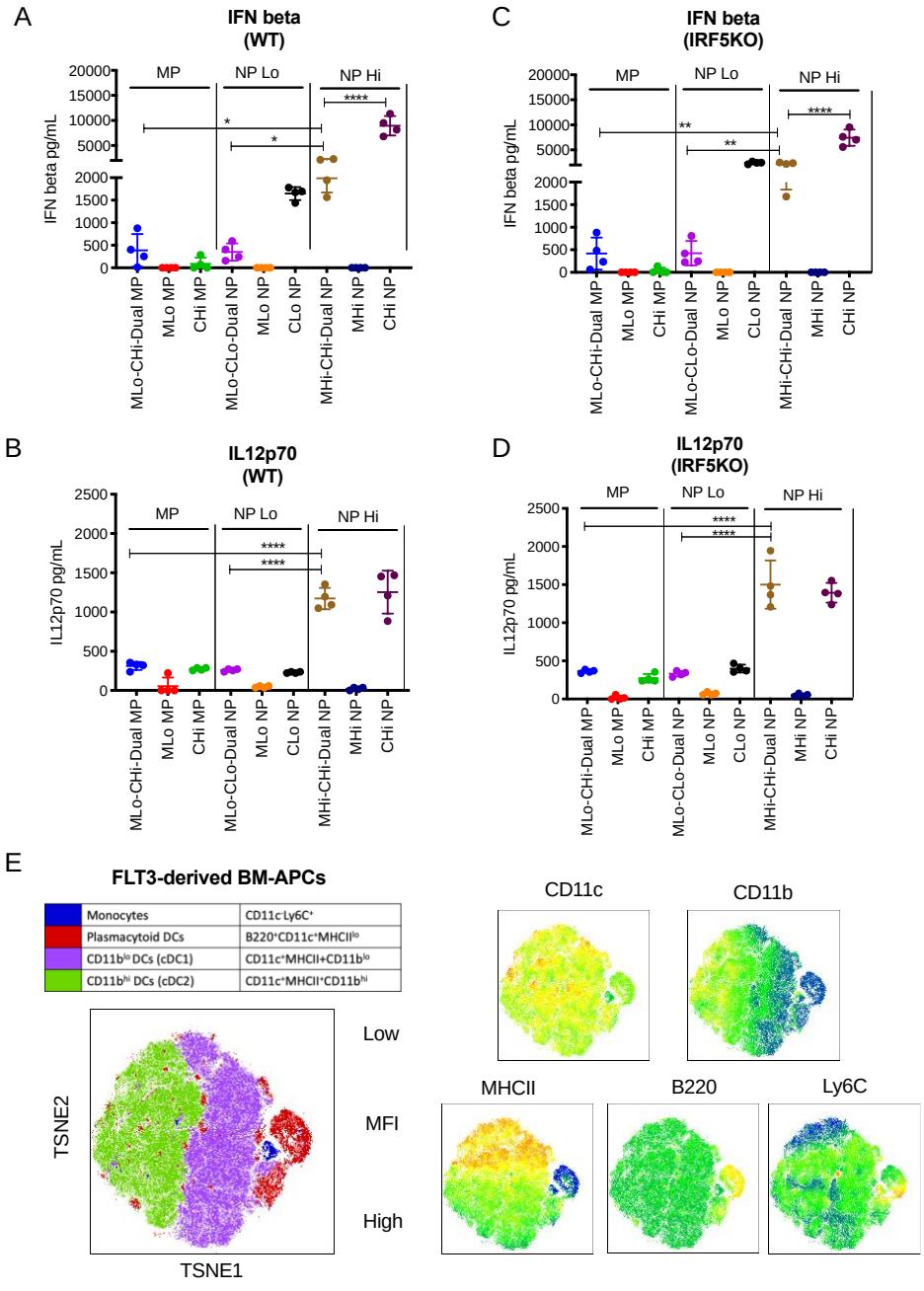

Figure S10. IFN-β and IL-12p70 responses of FLT3-derived BM-APCs from wild type and IRF-5$^{-/-}$ mice for MPLA-CpG PLPs. IFN-β (A and C) and IL-12p70 (B and D) responses of FLT3-derived BM-APCs from wild type (A-B) and IRF5 KO (C-D) mice following 24-hr activation with PLPs; E) Cellular subsets in FLT3-derived BM-APCs. Center lines designate the

mean value and error bars represent SD. *P < 0.05, **P < 0.01, ****P<0.0001; one-way ANOVA with Tukey's multiple comparison test.